arXiv:1009.0208v2 [cond-mat.stat-mech] 11 Mar 2011

Enskog Theory for Polydisperse Granular Mixtures. III. Comparison of dense and dilute transport coefficients and equations of state for a binary mixture

J. Aaron Murray and Christine M. Hrenya*
Department of Chemical and Biological Engineering, University of Colorado, Boulder, CO 80309

Vicente Garzó†
Departamento de Física, Universidad de Extremadura, E-06071 Badajoz, Spain

(Dated: March 14, 2011)

The objective of this study is to assess the impact of a dense-phase treatment on the hydrodynamic description of granular, binary mixtures relative to a previous dilute-phase treatment. Two theories were considered for this purpose. The first, proposed by Garzó and Dufty (GD) [Phys. Fluids **14**, 146 (2002)], is based on the Boltzmann equation which does not incorporate finite-volume effects, thereby limiting its use to dilute flows. The second, proposed by Garzó, Hrenya and Dufty (GHD) [Phys. Rev. E **76**, 31303 and 031304 (2007)], is derived from the Enskog equation which does account for finite-volume effects; accordingly this theory can be applied to moderately dense systems as well. To demonstrate the significance of the dense-phase treatment relative to its dilute counterpart, the ratio of dense (GHD) to dilute (GD) predictions of all relevant transport coefficients and equations of state are plotted over a range of physical parameters (volume fraction, coefficients of restitution, material density ratio, diameter ratio, and mixture composition). These plots reveal the deviation between the two treatments, which can become quite large (>100%) even at moderate values of the physical parameters. Such information will be useful when choosing which theory is most applicable to a given situation, since the dilute theory offers relative simplicity and the dense theory offers improved accuracy. It is also important to note that several corrections to original GHD expressions are presented here in the form of a complete, self-contained set of relevant equations.

I. INTRODUCTION

Polydisperse, rapid solids flows are quite prevalent in both nature (i.e., landslides, avalanches) and industry (i.e., pharmaceutical processing, high-velocity fluidized beds), though much remains to be understood. Perhaps most importantly, due to differences in size and/or material density of each particle species, polydisperse mixtures are well-known to exhibit particle segregation, also known as de-mixing [1–4]. Such behavior has no monodisperse counterpart. Thus, continuum models developed for monodisperse flows cannot be used to predict the segregation of unlike particles which occurs in polydisperse systems. Consequently, an accurate continuum model of a polydisperse solids mixture lends itself to a variety of non-trivial applications, such as the design of coal gasifiers for energy production.

The scope of the current study pertains to binary mixtures of inelastic grains (negligible fluid phase) engaging in instantaneous, binary collisions (rapid flows). Numerous previous contributors have proposed continuum theories for such systems (for recent review, see Ref. [5]), and the application of these theories has led to a better understanding of the mechanisms by which de-mixing occurs [3, 6–16]. Nevertheless, the improvement of existing models remains an active area of research due to differences in the derivation process. More specifically, one or both of the following simplifications have been incorporated in the vast majority of previous models: (i) Maxwellian velocity distribution [17–21], and/or (ii) an equipartition of energy [22, 23]. (The theories proposed by Rahaman *et al.* [20] as well as Iddir and Arastoopour [21] assumed a Maxwellian velocity distribution between unlike particles only.) The aforementioned assumptions are strictly true for systems of perfectly elastic spheres in a uniform steady state [24], but not so for inelastic grains. Furthermore, numerous studies have demonstrated the influence of non-equipartition on species segregation [7–9, 12–15]. Two continuum models have been proposed over the past decade in which neither of the above conditions is assumed. The first theory, developed by Garzó and Dufty (GD) [25–27] is based on the Boltzmann equation, and is thus applicable to dilute flows only. The second theory, developed recently by Garzó, Hrenya and Dufty (GHD) [28, 29], instead uses the Enskog equation as its starting point, making this theory applicable to moderately dense systems as well. Hereafter, the acronyms GD will be used to refer to the former, and GHD will be used to refer to latter. Each theory gives rise to a set of zeroth-order closures known as equations of state, as well as

---

*Electronic address: hrenya@colorado.edu
†Electronic address: vicenteg@unex.es; URL: `http://www.unex.es/eweb/fisteor/vicente/`

constitutive relations for first-order contributions to fluxes, or more specifically the associated transport coefficients. The equations of state and transport coefficients are functions of the hydrodynamic variables: number densities (n_i), mass-based mixture velocity ($\mathbf{U}$), and number-based mixture granular temperature (T). Although the predictions for the equations of state and transport coefficients from the two theories are expected to match at low volume fractions, a non-negligible difference is expected at higher concentrations, though the level of discrepancy between the two has not yet been reported for polydisperse systems.

To build on the previous contributions, the focus of this work is to analyze binary mixtures, where the two particle species differ in mass and/or size. Motivation for this study is threefold: (i) to assess importance of dense-phase corrections to hydrodynamic description of mixtures proposed by Garzó and co-workers [28, 29] compared to the previous dilute-phase description [25], and more specifically to determine rules-of-thumb for the volume fraction at which such dense-phase descriptions become non-negligible, (ii) to examine the behavior of the GHD equations of state and transport coefficients over a range of physical parameters, and (iii) to provide a complete, self-contained set of the GHD expressions, including several corrections (see the Appendix A) for the expressions given in the original GHD contribution [28, 29]. This latter goal also provides an opportunity to display the expressions in a form more suitable for computational purposes.

To accomplish the first two objectives, the equations of state and transport coefficients were evaluated over a range of volume fractions, coefficients of restitution, and mixture properties (diameter ratio, mass ratio, and volume fraction ratio). The results indicate that the discrepancy between transport coefficients and equations of state predicted by each theory at a volume fraction of $\phi = 0.1$ can vary from a factor of 1.05 to a factor of 10. As the volume fraction becomes fairly dense ($\phi = 0.5$), the predicted discrepancy increases to a factor of at least 1.7 and as large as a factor of 120. Hence, though the derivation of the constitutive relations for a dilute flow and the resulting constitutive expressions are simpler than its moderately dense counterpart, the difference between the two theories is non-negligible at low to moderate volume fractions. In the upcoming sections, a complete, self-contained set of the GHD constitutive relations for the mass flux, heat flux, pressure tensor, and cooling rate are given in Sections II. Also, a quantitative comparison between the GHD and GD predictions for the transport coefficients and equations of state illustrates stark differences between the dilute and dense treatments (Sections III and IV). The paper is closed in Sec. V with a brief summary of the main results obtained here.

II. ENSKOG KINETIC THEORY FOR MASS, MOMENTUM AND HEAT FLUXES AND EQUATIONS OF STATE OF A GRANULAR BINARY MIXTURE

The mass, momentum, and granular energy balances for the GHD theory for an s-component mixture are given in Table 1, along with the corresponding flux laws. Each balance equation is expressed in terms of the hydrodynamic variables (n_i, $\mathbf{U}$, T), along with the following quantities: cooling rate (ζ), mass flux ($\mathbf{j}_i$), heat flux ($\mathbf{q}$), and pressure tensor (P). Constitutive expressions for these latter quantities, also given in Table 1, are in terms of $\zeta^{(0)}$ (zeroth-order cooling rate), ζ_u (transport coefficient associated with first-order cooling rate), D_{ij} (mutual diffusion coefficients), D_i^T (thermal diffusion coefficients), D_{ij}^F (mass mobility), λ (thermal conductivity coefficient), $D_{q,i}$ (Dufour coefficients), L_{ij} (thermal mobility), p (pressure), η (shear viscosity), and κ (bulk viscosity). Also, $\mathbf{F}_i$ refers to the external force on a particle of species i. To fully close the set of equations, these quantities must be cast in terms of the hydrodynamic variables. The equations needed to obtain closures for each expression are detailed in the following subsections; corresponding equation numbers are also listed in Table 1.

A. Mass and heat fluxes

We consider a binary mixture ($s = 2$) of *inelastic*, smooth, hard disks ($d = 2$) or spheres ($d = 3$) of masses m_1 and m_2, and diameters σ_1 and σ_2. The inelasticity of collision among all pairs is characterized by three independent constant coefficients of normal restitution α_{11}, α_{22}, and $\alpha_{12} = \alpha_{21}$, where α_{ij} is the coefficient of restitution for collisions between particles of species i and j. For moderate densities, it is assumed that the velocity distribution functions of each species are accurately described by the coupled set of *inelastic* Enskog kinetic equations [30, 31]. This set of equations has been recently solved in Refs. [28, 29] by means of the Chapman-Enskog method [24] and the constitutive equations for the mass $\mathbf{j}_1$ and heat $\mathbf{q}$ fluxes have been obtained up to the Navier-Stokes order (first-order in the spatial gradients). In the absence of external forces ($\mathbf{F}_i = \mathbf{0}$), the forms of $\mathbf{j}_1$ and $\mathbf{q}$ are given, respectively, by

$$\mathbf{j}_1 = -\frac{m_1^2 n_1}{\rho} D_{11} \nabla \ln n_1 - \frac{m_1 m_2 n_2}{\rho} D_{12} \nabla \ln n_2 - \rho D_1^T \nabla \ln T, \tag{2.1}$$

$$\mathbf{q} = -T^2 D_{q,1} \nabla \ln n_1 - T^2 D_{q,2} \nabla \ln n_2 - \lambda \nabla T, \tag{2.2}$$

where $\rho = m_1 n_1 + m_2 n_2$ and n_i refers to the number density of species i. While the diffusion coefficients D_{ij} and the thermal diffusion coefficient D_i^T have only kinetic contributions, the transport coefficients $D_{q,i}$ and λ associated with the heat flux have also collisional transfer contributions. Expressions for these transport coefficients in terms of the coefficients of restitution, the parameters of the mixture (masses, sizes and composition), and concentration (solid volume fraction) have been obtained in Ref. [29] by using the leading terms in a Sonine polynomial expansion.

Table 1: Hydrodynamic description of a granular mixture from GHD theory.

Balance Equations	
Mass	$\frac{Dn_i}{Dt} + n_i \nabla \cdot \mathbf{U} = -\frac{1}{m_i} \nabla \cdot \mathbf{j}_i$
Momentum	$\rho \frac{D\mathbf{U}}{Dt} = -\nabla \cdot \mathbf{P} + \sum_{i=1}^{s} n_i \mathbf{F}_i$
Granular Energy	$\frac{d}{2} n \frac{DT}{Dt} = -\nabla \cdot \mathbf{q} - \mathbf{P} : \nabla \mathbf{U} - \frac{d}{2} n T \zeta + \frac{d}{2} T \sum_{i=1}^{s} \frac{1}{m_i} \nabla \cdot \mathbf{j}_i + \sum_{i=1}^{s} \frac{\mathbf{F}_i \cdot \mathbf{j}_i}{m_i}$

Flux Laws		
Mass	$\mathbf{j}_i = -\sum_{j=1}^{s} m_i m_j \frac{n_j}{\rho} D_{ij} \nabla \ln n_j - \rho D_i^T \nabla \ln T - \sum_{j=1}^{s} D_{ij}^F \mathbf{F}_j$	Eq. 2.1
Heat	$\mathbf{q} = -\lambda \nabla T - \sum_{i=1}^{s} T^2 D_{q,i} \nabla \ln n_i - \sum_{i=1}^{s} \sum_{j=1}^{s} L_{ij} \mathbf{F}_i$	Eq. 2.2
Pressure	$P_{\alpha\beta} = p\delta_{\alpha\beta} - \eta \left(\nabla_\alpha U_\beta + \nabla_\beta U_\alpha - \frac{2}{d} \nabla \cdot \mathbf{U} \delta_{\alpha\beta} \right) - \kappa \nabla \cdot \mathbf{U} \delta_{\alpha\beta}$	Eq. 2.22

Cooling Rate	$\zeta = \zeta^{(0)} + \zeta_u \nabla \cdot \mathbf{U}$

Equations of State			**Transport Coefficient**		
Zeroth-Order Cooling Rate	$\zeta^{(0)}$	Eq. 2.38	First-Order Cooling Rate	ζ_u	Eqs. 2.40, 2.41, 2.42
Pressure	p	Eqs. 2.24, 2.25	Shear Viscosity	η	Eqs. 2.27, 2.28, 2.30, 2.35
			Bulk Viscosity	κ	Eqs. 2.34, 2.36
			Mutual Diffusion	D_{ij}	Eqs. 2.3, 2.7, 2.8
			Thermal Diffusion	D_i^T	Eqs. 2.3, 2.6
			Thermal conductivity	λ	Eqs. 2.4, 2.13, 2.16, 2.17
			Dufour	$D_{q,i}$	Eqs. 2.4, 2.13, 2.15, 2.20
			Mass Mobility	D_{ij}^F	
			Thermal Mobility	L_{ij}	

The transport coefficients depend upon the temperature, concentration, and composition of the mixture, as well as the masses, diameters, and coefficients of restitution. To present the expressions of these coefficients in a compact form, it is convenient to consider their dimensionless forms:

$$D_{11}^* = \frac{m_1^2 \nu_0}{\rho T} D_{11}, \quad D_{12}^* = \frac{m_1 m_2 \nu_0}{\rho T} D_{12}, \quad D_1^{T*} = \frac{\rho \nu_0}{nT} D_1^T, \tag{2.3}$$

$$D_{q,i}^* = \frac{2}{d+2} \frac{(m_1+m_2)\nu_0}{n} D_{q,i}, \quad \lambda^* = \frac{2}{d+2} \frac{(m_1+m_2)\nu_0}{nT} \lambda. \tag{2.4}$$

Here, $\nu_0 = n\sigma_{12}^{d-1} v_0$ is an effective collision frequency, $\sigma_{12} = (\sigma_1+\sigma_2)/2$, and $v_0 = \sqrt{2T/m}$ is a thermal velocity where $m = (m_1+m_2)/2$. Thus, the results given throughout the remainder of the paper are given in terms of the mass ratio m_1/m_2, the size ratio σ_1/σ_2, the species number fraction $x_i = n_i/n$, the concentration $n\sigma_2^d$, and the coefficients of restitution α_{11}, α_{22}, and α_{12}.

A1. Mass flux transport coefficients

In a binary mixture, since $\mathbf{j}_1 = -\mathbf{j}_2$, the mass flux contains three relevant transport coefficients: D_{11}, D_{12}, and D_1^T. The remaining coefficients D_{22}, D_{21}, and D_2^T are given by the identities

$$D_{21} = -\frac{m_1}{m_2} D_{11}, \quad D_{22} = -\frac{m_1}{m_2} D_{12}, \quad D_2^T = -D_1^T. \tag{2.5}$$

The expressions of the reduced coefficients D_1^{T*}, D_{11}^*, and D_{12}^* can be written as [29]

$$\begin{aligned} D_1^{T*} &= (\nu_D^* - \zeta^*)^{-1} \Big\{ x_1\gamma_1 - \frac{p^*\rho_1}{\rho} + \frac{\pi^{d/2}}{2d\Gamma\left(\frac{d}{2}\right)} x_1 n\sigma_2^d \left[x_1\chi_{11}(\sigma_1/\sigma_2)^d \gamma_1 (1+\alpha_{11}) \right. \\ &\quad \left. + 2x_2\chi_{12}(\sigma_{12}/\sigma_2)^d M_{12}\gamma_2(1+\alpha_{12}) \right] \Big\}, \end{aligned} \tag{2.6}$$

$$\begin{aligned} \left(\nu_D^* - \frac{1}{2}\zeta^*\right) D_{11}^* &= \frac{D_1^{T*}}{x_1\nu_0} n_1 \frac{\partial \zeta^{(0)}}{\partial n_1} - \frac{m_1}{\rho T} n_1 \frac{\partial p}{\partial n_1} + \gamma_1 + n_1 \frac{\partial \gamma_1}{\partial n_1} \\ &\quad + \frac{\pi^{d/2}}{d\Gamma\left(\frac{d}{2}\right)} x_1 n\sigma_2^d \sum_{\ell=1}^{2} \chi_{1\ell}(\sigma_{1\ell}/\sigma_2)^d M_{\ell 1}(1+\alpha_{1\ell}) \\ &\quad \times \left\{ \frac{1}{2}\left(\gamma_1 + \frac{m_1}{m_\ell}\gamma_\ell\right) \left[2\delta_{1\ell} + n_\ell \frac{\partial \ln \chi_{1\ell}}{\partial n_1} + \frac{n_\ell}{n_1} I_{1\ell 1} \right] + \frac{m_1}{m_\ell} n_\ell \frac{\partial \gamma_\ell}{\partial n_1} \right\}, \end{aligned} \tag{2.7}$$

$$\begin{aligned} \left(\nu_D^* - \frac{1}{2}\zeta^*\right) D_{12}^* &= \frac{D_1^{T*}}{x_2\nu_0} n_2 \frac{\partial \zeta^{(0)}}{\partial n_2} - \frac{m_1}{\rho T} n_1 \frac{\partial p}{\partial n_2} + n_1 \frac{\partial \gamma_1}{\partial n_2} \\ &\quad + \frac{\pi^{d/2}}{d\Gamma\left(\frac{d}{2}\right)} x_1 n\sigma_2^d \sum_{\ell=1}^{2} \chi_{1\ell}(\sigma_{1\ell}/\sigma_2)^d M_{\ell 1}(1+\alpha_{1\ell}) \\ &\quad \times \left\{ \frac{1}{2}\left(\gamma_1 + \frac{m_1}{m_\ell}\gamma_\ell\right) \left[2\delta_{2\ell} + n_\ell \frac{\partial \ln \chi_{1\ell}}{\partial n_2} + \frac{n_\ell}{n_2} I_{1\ell 2} \right] + \frac{m_1}{m_\ell} n_\ell \frac{\partial \gamma_\ell}{\partial n_2} \right\}. \end{aligned} \tag{2.8}$$

In these equations, $\rho_i = m_i n_i$, $\gamma_i = T_i/T$, $\zeta^* = \zeta^{(0)}/\nu_0$, $p^* = p/(nT)$, χ_{ij} is the pair distribution function at contact, $M_{ij} = m_i/(m_i+m_j)$, and

$$\nu_D^* = \frac{\sqrt{2}\pi^{(d-1)/2}}{d\Gamma\left(\frac{d}{2}\right)} \chi_{12}(1+\alpha_{12}) \left(\frac{\gamma_1}{M_{12}} + \frac{\gamma_2}{M_{21}}\right)^{1/2} (x_1 M_{12} + x_2 M_{21}). \tag{2.9}$$

The partial temperatures T_1 and T_2 are determined from the condition $\zeta_1^{(0)} = \zeta_2^{(0)} = \zeta^{(0)}$, where the expression of $\zeta_i^{(0)}$ is given by Eq. (2.38). Moreover, an explicit form for χ_{ij} for disks ($d=2$) and spheres ($d=3$) is given in the Appendix B.

The parameters $I_{i\ell j}$ are chosen to recover the results derived by López de Haro *et al.* for elastic mixtures [32]. These quantities are the origin of the primary difference between the standard Enskog theory and the revised version for elastic collisions [33]. They are zero if $i = \ell$, but otherwise are not zero. They are defined through the relation [29]

$$\sum_{\ell=1}^{2} n_\ell \sigma_{i\ell}^d \chi_{i\ell} \left(n_j \frac{\partial \ln \chi_{i\ell}}{\partial n_j} + I_{i\ell j} \right) = \frac{n_j}{TB_2} \left(\frac{\partial \mu_i}{\partial n_j} \right)_{T, n_{k\neq j}} - \frac{\delta_{ij}}{B_2} - 2 n_j \chi_{ij} \sigma_{ij}^d. \tag{2.10}$$

where $B_2 = \pi^{d/2}/d\Gamma\left(d/2\right)$ [Γ refers to Gamma function, such that $B_2 = \frac{\pi}{2}$ for $d = 2$ (disks) and $B_2 = 2\pi/3$ for $d = 3$ (spheres)] and μ_i is the chemical potential of species i. Taking into account Eq. (2.10), the nonzero parameters I_{121} and I_{122} appearing in Eqs. (2.11) and (2.12) are given by

$$I_{121} = \frac{1}{TB_2 n_2 \sigma_{12}^d \chi_{12}} \left[n_1 \left(\frac{\partial \mu_1}{\partial n_1} \right)_{T, n_2} - T \right] - 2 \frac{n_1 \sigma_1^d \chi_{11}}{n_2 \sigma_{12}^d \chi_{12}} - \frac{n_1^2 \sigma_1^d}{n_2 \sigma_{12}^d \chi_{12}} \frac{\partial \chi_{11}}{\partial n_1} - \frac{n_1}{\chi_{12}} \frac{\partial \chi_{12}}{\partial n_1}, \tag{2.11}$$

$$I_{122} = \frac{1}{TB_2 \sigma_{12}^d \chi_{12}} \left(\frac{\partial \mu_1}{\partial n_2} \right)_{T, n_1} - 2 - \frac{\sigma_1^d n_1}{\sigma_{12}^d \chi_{12}} \frac{\partial \chi_{11}}{\partial n_2} - \frac{n_2}{\chi_{12}} \frac{\partial \chi_{12}}{\partial n_2}. \tag{2.12}$$

Explicit forms of μ_i for disks ($d = 2$) and spheres ($d = 3$) are given in the Appendix B.

A2. Heat flux transport coefficients

The heat flux requires going up to the second Sonine approximation. Its constitutive equation is given by Eq. (2.2) where the transport coefficients $D_{q,i}$ and λ have kinetic and collisional contributions

$$D_{q,i} = D_{q,i}^k + D_{q,i}^c, \quad \lambda = \lambda^k + \lambda^c. \tag{2.13}$$

The corresponding reduced forms $D_{q,i}^{k*}$, $D_{q,i}^{c*}$, λ^{k*}, and λ^{c*} are defined as

$$D_{q,i}^{k,c*} = \frac{2}{d+2} \frac{(m_1 + m_2)\nu_0}{n} D_{q,i}^{k,c}, \quad \lambda^{k,c*} = \frac{2}{d+2} \frac{(m_1 + m_2)\nu_0}{nT} \lambda^{k,c}. \tag{2.14}$$

The kinetic parts $D_{q,i}^{k*}$ and λ^{k*} can be written, respectively, as

$$D_{q,1}^{k*} = d_{q,11}^* + d_{q,21}^* + \left(\frac{\gamma_1}{M_{12}} - \frac{\gamma_2}{M_{21}} \right) x_1 D_{11}^*, \quad D_{q,2}^{k*} = d_{q,22}^* + d_{q,12}^* + \left(\frac{\gamma_1}{M_{12}} - \frac{\gamma_2}{M_{21}} \right) x_2 D_{12}^*, \tag{2.15}$$

$$\lambda^{k*} = \lambda_1^* + \lambda_2^* + \left(\frac{\gamma_1}{M_{12}} - \frac{\gamma_2}{M_{21}} \right) D_1^{T*}, \tag{2.16}$$

where the expressions for the (dimensionless) coefficients $d_{q,ij}^*$ and λ_i^* are displayed in the Appendix B. In Eqs. (2.15) and (2.16), the coefficients D_1^{T*}, D_{11}^* and D_{12}^* are given by Eqs. (2.6), (2.7), and (2.8), respectively (first Sonine approximation).

Let us consider now their collisional transfer contributions. In the case of the thermal conductivity, λ^{c*} is given by [29]

$$\begin{aligned} \lambda^{c*} = {} & \frac{3}{2} \frac{\pi^{d/2}}{d(d+2)\Gamma\left(\frac{d}{2}\right)} n\sigma_2^d \sum_{i=1}^{2} \sum_{j=1}^{2} x_i (\sigma_{ij}/\sigma_2)^d \chi_{ij} M_{ij} (1 + \alpha_{ij}) \left\{ \left[(5 - \alpha_{ij}) M_{ij} - (1 - \alpha_{ij}) M_{ji} \right] \lambda_j^* \right. \\ & + (m_1 + m_2) D_j^{T*} \left[\frac{\gamma_j}{m_j} \left((5 - \alpha_{ij}) M_{ij} - (1 - \alpha_{ij}) M_{ji} \right) + \frac{\gamma_i}{m_i} \left((3 + \alpha_{ij}) M_{ji} - (7 + \alpha_{ij}) M_{ij} \right) \right] \\ & \left. + \frac{16}{3\sqrt{\pi}} \frac{x_j m_j}{m_1 + m_2} (\sigma_{12}/\sigma_2)^d (\sigma_{ij}/\sigma_{12}) C_{ij}^* \right\}, \end{aligned} \tag{2.17}$$

where

$$\begin{aligned} C^*_{ij} &= (\theta_i+\theta_j)^{-1/2}(\theta_i\theta_j)^{-3/2}\left\{2\beta_{ij}^2+\theta_i\theta_j+(\theta_i+\theta_j)\left[(\theta_i+\theta_j)M_{ij}M_{ji}+\beta_{ij}(1+M_{ji})\right]\right\} \\ &\quad +\frac{3}{4}(1-\alpha_{ij})(M_{ji}-M_{ij})\left(\frac{\theta_i+\theta_j}{\theta_i\theta_j}\right)^{3/2}\left[M_{ji}+\beta_{ij}(\theta_i+\theta_j)^{-1}\right]. \end{aligned} \tag{2.18}$$

Here, $\theta_i = (m_i T/mT_i)$ and $\beta_{ij} = M_{ij}\theta_j - M_{ji}\theta_i$. In the case of the coefficients $D^{c*}_{q,i}$, they can be written as [29]

$$D^{c*}_{q,1} = D^{c*}_{q,11} + D^{c*}_{q,21}, \quad D^{c*}_{q,2} = D^{c*}_{q,12} + D^{c*}_{q,22}, \tag{2.19}$$

where the coefficients $D^{c*}_{q,ij}$ have the explicit forms

$$\begin{aligned} D^{c*}_{q,ij} &= \frac{3}{2}\frac{\pi^{d/2}}{d(d+2)\Gamma\left(\frac{d}{2}\right)}n\sigma_2^d\sum_{p=1}^{2}x_p(\sigma_{ip}/\sigma_{12})^d\chi_{ip}M_{ip}(1+\alpha_{ip})\Big\{\left[(5-\alpha_{ij})M_{ip}-(1-\alpha_{ij})M_{pi}\right]d^*_{q,pj} \\ &\quad +(m_1+m_2)x_jD^*_{pj}\left[\frac{\gamma_p}{m_p}\left((5-\alpha_{ip})M_{ip}-(1-\alpha_{ip})M_{pi}\right)\right. \\ &\quad \left.+\frac{\gamma_i}{m_i}\left((3+\alpha_{ip})M_{pi}-(7+\alpha_{ip})M_{ip}\right)\right]-\frac{32}{3\sqrt{\pi}}\frac{x_pm_p}{m_1+m_2}(\sigma_{12}/\sigma_2)^d(\sigma_{ip}/\sigma_{12})C^*_{ipj}\Big\}, \end{aligned} \tag{2.20}$$

where

$$\begin{aligned} C^*_{ipj} &= (\theta_i+\theta_p)^{-1/2}(\theta_i\theta_p)^{-3/2}\left\{\delta_{jp}\beta_{ip}(\theta_i+\theta_p)-\frac{1}{2}\theta_i\theta_p\left[1+\frac{M_{pi}(\theta_i+\theta_p)-2\beta_{ip}}{\theta_p}\right]\frac{\partial\ln\gamma_p}{\partial\ln n_j}\right\} \\ &\quad +\frac{1}{4}(1-\alpha_{ip})(M_{pi}-M_{ip})\left(\frac{\theta_i+\theta_p}{\theta_i\theta_p}\right)^{3/2}\left(\delta_{jp}+\frac{3}{2}\frac{\theta_i}{\theta_i+\theta_p}\frac{\partial\ln\gamma_p}{\partial\ln n_j}\right). \end{aligned} \tag{2.21}$$

B. Pressure tensor

The overall constitutive relation for the pressure tensor is a combination of the zeroth ($\mathbf{P}^{(0)}$) and first-order ($\mathbf{P}^{(1)}$) contributions, which is given by

$$\mathbf{P} = \mathbf{P}^{(0)} + \mathbf{P}^{(1)} \tag{2.22}$$

where

$$P^{(0)}_{\alpha\beta} = p\delta_{\alpha\beta}. \tag{2.23}$$

The zeroth-order contribution to the pressure tensor is proportional to the mixture granular pressure p. The equation of state that defines p is given by

$$p = p^k + p^c \tag{2.24}$$

where the kinetic (p^k) and the collisional (p^c) contributions are [28]

$$p^k = nT \quad , \quad p^c = \frac{\pi^{d/2}}{d\Gamma\left(\frac{d}{2}\right)}p^k\, n\sigma_2^d\sum_{i=1}^{2}\sum_{j=1}^{2}\, x_ix_j(\sigma_{ij}/\sigma_2)^dM_{ji}\left(1+\alpha_{ij}\right)\chi_{ij}\gamma_i. \tag{2.25}$$

The constitutive equation for the pressure tensor $P^{(1)}_{\alpha\beta}$, proportional to the velocity gradients, is

$$P^{(1)}_{\alpha\beta} = -\eta\left(\nabla_\alpha U_\beta + \nabla_\beta U_\alpha - \frac{2}{d}\nabla\cdot\mathbf{U}\delta_{\alpha\beta}\right) - \kappa\nabla\cdot\mathbf{U}\delta_{\alpha\beta}. \tag{2.26}$$

Here, η is the shear viscosity and κ is the bulk viscosity. The coefficient η has kinetic and collisional contributions while κ only has a collisional contribution κ^c (and so, vanishes for dilute gases)

$$\eta = \eta^k + \eta^c, \quad \kappa = \kappa^c. \tag{2.27}$$

The kinetic part η^k is

$$\eta^k = \eta_1^k + \eta_2^k, \tag{2.28}$$

where the partial contributions η_i^k can be written as

$$\eta_i^k = \frac{nT}{\nu_0}\eta_i^{k*}. \tag{2.29}$$

The reduced coefficients η_i^{k*} are given by

$$\eta_1^{k*} = \frac{2(2\tau_{22}^* - 2\zeta^*)\overline{\eta}_1 - 4\tau_{12}^*\overline{\eta}_2}{\zeta^{*2} - 2\zeta^*(\tau_{11}^* + \tau_{22}^*) + 4(\tau_{11}^*\tau_{22}^* - \tau_{12}^*\tau_{21}^*)}, \tag{2.30}$$

$$\eta_2^{k*} = \frac{2(2\tau_{11}^* - 2\zeta^*)\overline{\eta}_2 - 4\tau_{21}^*\overline{\eta}_1}{\zeta^{*2} - 2\zeta^*(\tau_{11}^* + \tau_{22}^*) + 4(\tau_{11}^*\tau_{22}^* - \tau_{12}^*\tau_{21}^*)}, \tag{2.31}$$

where the expressions of the (reduced) collision frequencies τ_{ij}^* can be found in the Appendix A of Ref. [29]. In Eq. (2.30), we have introduced the quantities

$$\overline{\eta}_1 = x_1\gamma_1 + E_{11} + E_{12}, \quad \overline{\eta}_2 = x_2\gamma_2 + E_{22} + E_{21}, \tag{2.32}$$

where

$$\begin{aligned} E_{ij} &= \frac{\pi^{d/2}}{d(d+2)\Gamma\left(\frac{d}{2}\right)} n\sigma_2^d x_i x_j (\sigma_{ij}/\sigma_2)^d \chi_{ij} M_{ji}(1+\alpha_{ij}) \\ &\quad \times \left[M_{ji}(3\alpha_{ij}-1)\left(\gamma_i + \frac{m_i}{m_j}\gamma_j\right) - 4M_{ij}(\gamma_i - \gamma_j)\right]. \end{aligned} \tag{2.33}$$

The collisional contribution η^c to the shear viscosity and the the bulk viscosity κ have the forms

$$\eta^c = \frac{nT}{\nu_0}\eta^{c*}, \quad \kappa = \frac{nT}{\nu_0}\kappa^*, \tag{2.34}$$

where

$$\eta^{c*} = \frac{2\pi^{d/2}}{\Gamma\left(\frac{d}{2}\right)} \frac{1}{d(d+2)} n\sigma_2^d \sum_{i=1}^2 \sum_{j=1}^2 x_j (\sigma_{ij}/\sigma_2)^d \chi_{ij} M_{ji}(1+\alpha_{ij})\eta_i^{k*} + \frac{d}{d+2}\kappa^*, \tag{2.35}$$

$$\kappa^* = \frac{4\pi^{(d-1)/2}}{d^2\Gamma\left(\frac{d}{2}\right)} \frac{(n\sigma_2^d)^2}{m_1+m_2} \sum_{i=1}^2 \sum_{j=1}^2 x_i x_j \frac{m_i m_j}{m_i + m_j} \frac{\sigma_{12}^{d-1}\sigma_{ij}^{d+1}}{\sigma_2^{2d}} \chi_{ij}(1+\alpha_{ij}) \left(\frac{\theta_i+\theta_j}{\theta_i\theta_j}\right)^{1/2}. \tag{2.36}$$

It must be remarked that the predictions of the shear viscosity η compare quite well with Monte Carlo simulations of a heated granular binary mixture, even for strong dissipation [34].

C. Cooling rate

The overall cooling rate can be written as the sum of the zeroth-order ($\zeta^{(0)}$) and first-order contributions (ζ_u)

$$\zeta = \zeta^{(0)} + \zeta_u \nabla \cdot \mathbf{U}. \tag{2.37}$$

The zeroth-order cooling rate of each species ($\zeta_i^{(0)}$) defines the rate of kinetic energy loss for that species, and is given by the following relation

$$\begin{aligned} \zeta^{(0)} = \zeta_i^{(0)} &= \frac{4\pi^{(d-1)/2}}{d\Gamma\left(\frac{d}{2}\right)} \nu_0 \sum_{j=1}^2 \chi_{ij} x_j M_{ji} (\sigma_{ij}/\sigma_{12})^{d-1} \left(\frac{\theta_i+\theta_j}{\theta_i\theta_j}\right)^{1/2} (1+\alpha_{ij}) \\ &\quad \times \left[1 - \frac{M_{ji}}{2}(1+\alpha_{ij})\frac{\theta_i+\theta_j}{\theta_j}\right]. \end{aligned} \tag{2.38}$$

As shown in Eq. (2.38), the zeroth-order cooling rate for each species is equivalent (i.e., $\zeta_1^{(0)}=\zeta_2^{(0)}$). Because Eq. (2.38) is an implicit expression that depends on individual species granular temperatures, the following equation is needed

$$nT=n_1T_1+n_2T_2. \tag{2.39}$$

The expressions given in Eq. (2.38) and Eq. (2.39) form a set of two non-linear algebraic equations that can be solved for θ_1 and θ_2 (using the relation $\theta_i=m_iT/mT_i$), and then species temperatures T_1 and T_2 can subsequently be found. The equation of state defining $\zeta^{(0)}$ was first proposed by Garzó and Dufty [35].

At first order in gradients, there is a contribution to the cooling rate from $\nabla\cdot\mathbf{U}$. The proportionality coefficient ζ_u is a new transport coefficient for granular fluids. Two different contributions can be identified

$$\zeta_u=\zeta^{(1,0)}+\zeta^{(1,1)}. \tag{2.40}$$

The coefficient $\zeta^{(1,0)}$ is given by

$$\zeta^{(1,0)}=-\frac{3\pi^{d/2}}{d^2\Gamma\left(\frac{d}{2}\right)}n\sigma_2^d\sum_{i=1}^{2}\sum_{j=1}^{2}x_ix_jM_{ji}(\sigma_{ij}/\sigma_2)^d\chi_{ij}(1-\alpha_{ij}^2)\gamma_i. \tag{2.41}$$

The contribution $\zeta^{(1,1)}$ can be written as

$$\zeta^{(1,1)}=\frac{3\pi^{(d-1)/2}}{d\Gamma\left(\frac{d}{2}\right)}\sum_{i=1}^{2}\sum_{j=1}^{2}\frac{m_j}{m_1+m_2}x_ix_j(\sigma_{ij}/\sigma_{12})^{d-1}\chi_{ij}M_{ij}(1-\alpha_{ij}^2)\theta_i^{-3/2}\theta_j^{1/2}(\theta_i+\theta_j)^{-1/2}e_{i,D}^*, \tag{2.42}$$

where

$$e_{1,D}^*=\frac{2(2\psi_{22}^*-3\zeta^*)\overline{e}_{1,D}-4\psi_{12}^*\overline{e}_{2,D}}{9\zeta^{*2}-6\zeta^*(\psi_{11}^*+\psi_{22}^*)+4(\psi_{11}^*\psi_{22}^*-\psi_{12}^*\psi_{21}^*)}, \tag{2.43}$$

$$e_{2,D}^*=\frac{2(2\psi_{11}^*-3\zeta^*)\overline{e}_{2,D}-4\psi_{21}^*\overline{e}_{1,D}}{9\zeta^{*2}-6\zeta^*(\psi_{11}^*+\psi_{22}^*)+4(\psi_{11}^*\psi_{22}^*-\psi_{12}^*\psi_{21}^*)}. \tag{2.44}$$

Here, the collision frequencies ψ_{ij}^* have been determined in the Appendix A of Ref. [29] and the coefficients $\overline{e}_{i,D}$ are given by

$$\begin{aligned}\overline{e}_{i,D} \;=\; &-\frac{\pi^{d/2}}{2d^2(d+2)\Gamma\left(\frac{d}{2}\right)}n\sigma_2^d\sum_{j=1}^{2}x_j(\sigma_{ij}/\sigma_{12})^d\chi_{ij}M_{ji}(1+\alpha_{ij})\left[8(d+2)(M_{ij}-1)\right.\\ &+4(13+2d+9\alpha_{ij})M_{ji}-48M_{ji}^2\theta_j^{-1}(\theta_i+\theta_j)(1+\alpha_{ij})^2\\ &\left.+15M_{ji}^3\theta_j^{-2}(\theta_i+\theta_j)^2(1+\alpha_{ij})^3\right].\end{aligned} \tag{2.45}$$

The results displayed along this section give the explicit forms for the equations of state, the transport coefficients and the cooling rate of a moderately dense granular binary mixture. The corresponding expressions for a low-density binary mixture can be easily obtained from their dense forms by taking the limit $n\sigma_2^d\to 0$. These explicit expressions are displayed in the Appendix C and agree with those previously derived from the Boltzmann equation [25, 27].

III. QUANTITATIVE APPROACH: COMPARISON OF DILUTE AND DENSE-PHASE EXPRESSIONS FOR HARD SPHERES

In order to assess the importance of dense-phase corrections to the continuum theory for rapid granular flows of binary mixtures, the equations of state and transport coefficients obtained from the GHD and GD theories were compared over a range of volume fractions and coefficients of restitution for a given set of mixture properties (diameter ratio, size ratio, and volume fraction ratio). To illustrate the differences in a straightforward manner, each quantity is examined as a ratio of the GHD value (dilute through moderately dense) to the GD value (dilute limit), giving rise to a non-dimensional quantity. These non-dimensional ratios were plotted as functions of volume fraction and coefficients of restitution, holding all other mixture properties constant. Representing the transport coefficients and equations of state in this manner reveals the relative magnitudes of the dense- and dilute-phase predictions. Recall the complete set of equations of state and transport coefficients for GHD theory are given in Table 1 ($\zeta^{(0)}$, ζ_u, D_{ij}, D_i^T, D_{ij}^F, λ, $D_{q,i}$, L_{ij}, p, η, κ).

It is important to note that some transport coefficients (L_{ij}, D_{ij}^F) were not considered in the dilute theory (GD), and thus these quantities are not considered here. Moreover, two of the transport coefficients, namely ζ_u and κ, are zero in the dilute limit, and thus the corresponding ratios of the moderately dense (GHD) value to the dilute (GD) value diverge. Accordingly, only the GHD predictions of these quantities are shown. Thus, the comparison between the GHD and GD theory predictions presented here involves the seven remaining quantities: $\zeta^{(0)}$, p, η, D_{ij}, D_i^T, λ, $D_{q,i}$.

A. Mixture parameters

The continuum description of a binary mixture of inelastic hard spheres ($d = 3$) is a function of the following dimensional parameters: species masses (m_1, m_2), species diameters (σ_1, σ_2), species 1 volume fraction (ϕ_1), overall volume fraction ($\phi = \phi_1 + \phi_2$), and coefficients of restitution ($\alpha_{11}, \alpha_{22}, \alpha_{12} = \alpha_{21}$). (Note that the number densities and volume fractions are related by $\phi_i = n_i \pi \sigma_i^3/6$.) The subscripts 1 and 2 denote the two species in the binary mixture. For purposes of simplicity, the coefficients of restitution have been assumed to be the same for all combinations of collisions (i.e., $\alpha_{11} = \alpha_{22} = \alpha_{12} \equiv \alpha$). In terms of the ratio of moderately dense (GHD) to dilute (GD) predictions for each quantity, the parameter space is reduced to the following dimensionless inputs: mass ratio (m_1/m_2), diameter ratio (σ_1/σ_2), overall volume fraction (ϕ), volume fraction ratio of species 1 relative to the total (ϕ_1/ϕ), and coefficient of restitution α. Hereafter, the ratio ϕ_1/ϕ will be referred to as the (mixture) composition of species 1. Recall that the GHD and GD theories allow for a non-equipartition of energy, and thus several of the aforementioned closures (see, for example, Eq. (2.15)) involve the species granular temperatures, T_1 and T_2. It is important to point out that these quantities are not hydrodynamic variables (i.e., they do not require the solution of species energy balances; for a detailed explanation, see Ref. [29]) and instead are determined by the set of equations defining the zeroth-order cooling rate (Eqs. (2.37) and (2.38)).

B. Parameter space evaluated

Table 2 summarizes the three cases (equal size and different mass, equal mass and different size, and different size and mass) used to compare the GHD and GD theories, and the wide ranges of input parameters used in each case study. Though the transport coefficients and equations of state may vary quantitatively from case to case, the general trends show little variation. For sake of brevity, the upcoming section will focus on one representative case, namely that of different size and equal material densities (i.e., different mass) in order to quantify how the newly acquired GHD predictions differ from the dilute-phase counterpart (GD).

Table 2: Range of input parameters used in analysis of binary mixture via GHD theory

Case Description	σ_1/σ_2	m_1/m_2	ϕ_1/ϕ	α
Equal Sizes	1	1-10	0.25-0.75	0.50-0.99
Equal Masses	1-10	1	0.25-0.75	0.50-0.99
Different diameters, different masses	2	0.10-10	0.50	0.75

C. Case presented: Different-sized particles with equal material densities

Many industrial and natural granular flows are comprised of one material (i.e., same material density), but different-sized particles. In the case presented here, the diameter of species 1 was twice that of species 2 (i.e., $\sigma_1/\sigma_2 = 2$), and both species had the same material density (i.e., $m_1/m_2 = 8$). For the sake of consistency, the composition of each species was held constant at 50% by volume for this analysis (i.e., $\phi_1/\phi = \phi_2/\phi = 0.5$). The ratio of GHD to GD predictions of each quantity evaluated was plotted over a range of volume fractions from dilute to moderately dense ($\phi = 10^{-8}$-0.5) while holding the coefficient of restitution constant. Also, each quantity was varied over a range of coefficients of restitution from relatively inelastic to nearly elastic (0.5-0.99) while holding the overall volume fraction constant. The results of this case study are presented in the upcoming section.

IV. RESULTS AND DISCUSSION

The overall objective was to analyze each transport coefficient and equation of state over a range of parameters for the newly-developed GHD theory. By comparing these results to the predictions from the dilute (GD) theory, it was possible to demonstrate the need for a moderately dense-phase correction, as detailed below.

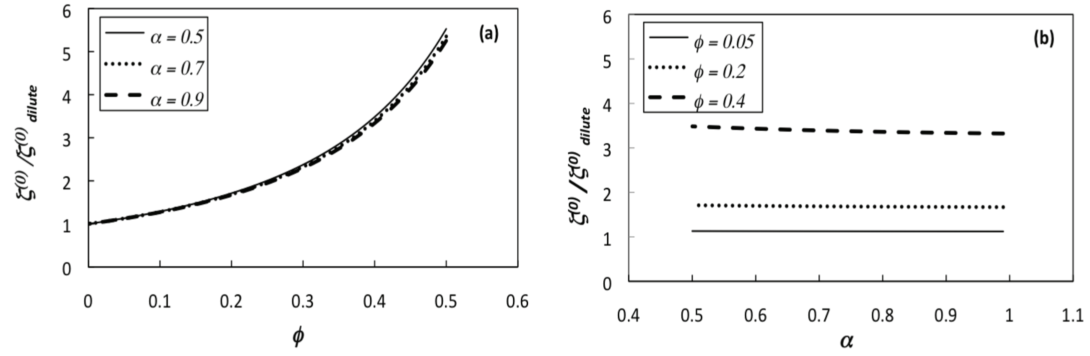

FIG. 1: Zeroth-order cooling rate: ratio of moderately dense (GHD) to dilute (GD) predictions as a function of (a) overall volume fraction and (b) coefficient of restitution.

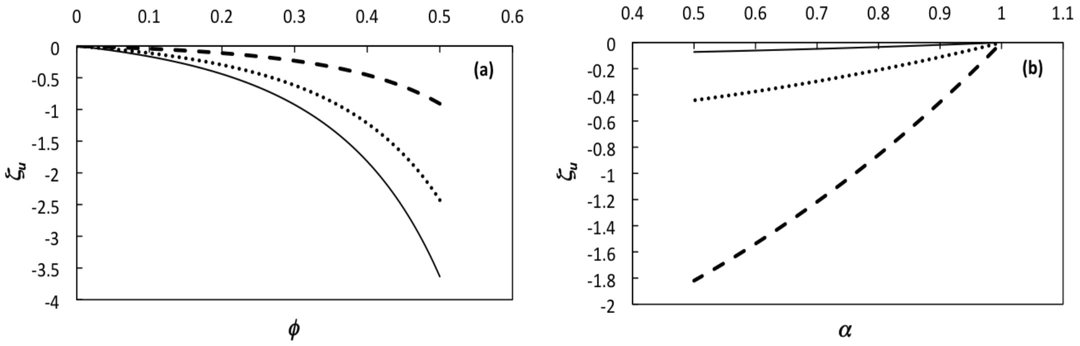

FIG. 2: Transport coefficient associated with first-order cooling rate: moderately dense (GHD) predictions as a function of (a) overall volume fraction and (b) coefficient of restitution. See legends presented in Figure 1.

A. Cooling rate: zeroth-order and first-order contributions

As indicated by Figure 1, the dense-to-dilute ratio of the zeroth-order cooling rate ($\zeta^{(0)}$) is much more sensitive to changes in volume fraction than coefficient of restitution. Such behavior can be explained via the dependency of the zeroth-order cooling rate (Eq. 2.38) on the pair correlation function at contact, χ_{ij} (Eqs. (B14) and (B17)). This factor accounts for the volume exclusion effects between like particles (χ_{11}) and unlike particles (χ_{12}). In the dilute limit, the spatial correlation factor equals one (i.e., $\chi_{11} = \chi_{12} = 1$). When the zeroth-order cooling rate of GHD theory is then divided by its dilute counterpart, the resulting function is strongly dependent on the spatial correlation factor. Because χ_{ij} is sensitive to changes in overall volume fraction, it is then reasonable that the dimensionless zeroth-order cooling rate ratio exhibits the same sensitivity. More specifically, the results shown in Figure 1a indicate that $\zeta^{(0)}$ predicted by GHD theory is more than 5 times greater than its dilute counterpart for a fairly dense system ($\phi = 0.5$) and more than 2 times greater for $\phi = 0.3$. Even at $\phi = 0.2$, a discrepancy of 27% is found between the dilute- and dense-phase predictions.

Unlike the zeroth-order contribution to the cooling rate, the transport coefficient associated with the first-order contribution is zero in the dilute limit. Therefore, a ratio comparison of the dense-to-dilute predictions is not possible. The results given in Figure 2 represent the first-order contribution to the cooling rate (which is non-dimensional), which approaches zero as volume fraction diminishes. As evident from this figure, ζ_u is quite sensitive to changes in both volume fraction (Fig. 2a) and coefficient of restitution (Fig. 2b). Also, the results for this case indicate that the magnitude of the first-order contribution increases as the system becomes denser and less elastic.

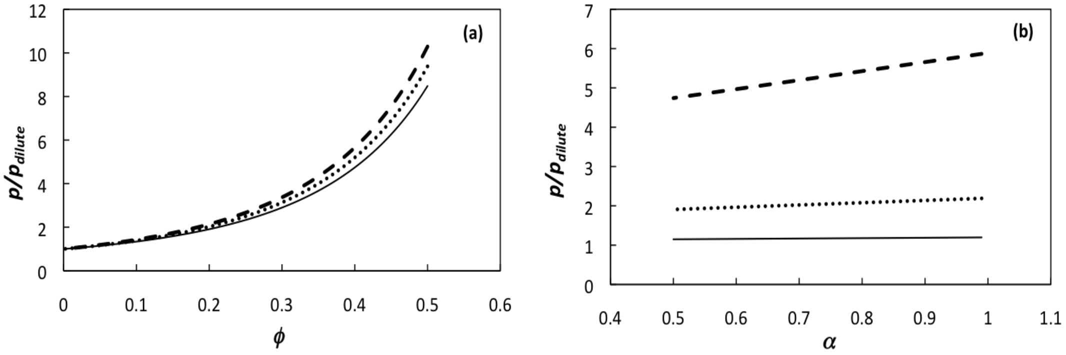

FIG. 3: Pressure: ratio of moderately dense (GHD) to dilute (GD) predictions as a function of (a) overall volume fraction and (b) coefficient of restitution. See legends presented in Figure 1.

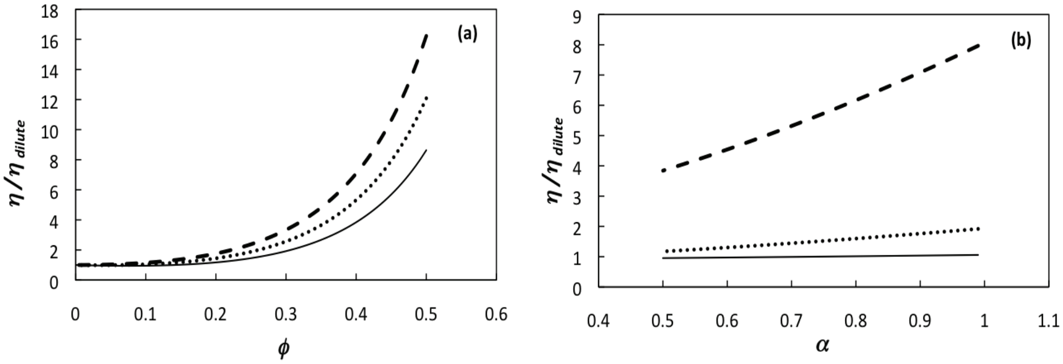

FIG. 4: Shear viscosity: ratio of moderately dense (GHD) to dilute (GD) predictions as a function of (a) overall volume fraction and (b) coefficient of restitution. See legends presented in Figure 1.

B. Momentum flux: pressure, shear viscosity and bulk viscosity

Now moving on to results associated with the momentum flux, Figure 3 indicates that the dense-to-dilute ratio of granular pressure is more sensitive to changes in volume fraction (Fig. 3a) than coefficient of restitution (Fig. 3b). Also, this ratio increases monotonically with both volume fraction and coefficient of restitution. For a moderately dense system ($\phi \sim 0.4$), GHD theory predicts that the granular pressure is about 5 times greater than dilute (GD) theory. Even at lower volume fractions ($\phi \sim 0.1$), the moderately dense-phase prediction is greater than its dilute counterpart by 40%.

Shear viscosity, results of which are given in Figure 4, behaves in a similar manner to granular pressure (Fig. 3). A monotonic increase is exhibited with respect to both volume fraction (Fig. 4a) and coefficient of restitution (Fig. 4b). The GHD prediction is about 5 times larger than the GD prediction for moderately dense systems ($\phi \sim 0.4$). However, the discrepancy at lower volume fractions ($\phi \sim 0.1$) decreases to approximately 5% (Fig. 4a).

As mentioned previously, the bulk viscosity is zero in the dilute limit. Therefore the results for bulk viscosity, given in Figure 5, are those obtained from the moderately dense theory (GHD) alone, instead ratios of dense-to-dilute predictions. Furthermore, these GHD-based bulk viscosities are non-dimensionalized according to Eqs. (2.34) and (2.36). It is evident from this figure that the prediction of bulk viscosity via GHD theory increases significantly in magnitude as the system becomes moderately dense, whereas little variation results from changes in particle elasticity.

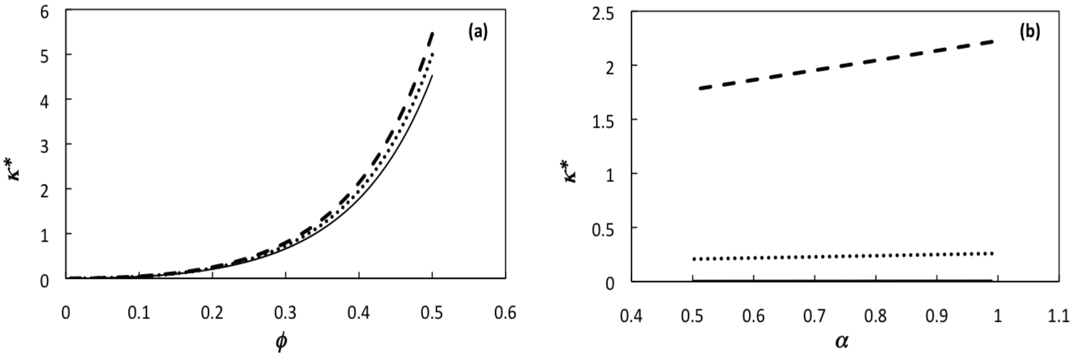

FIG. 5: Bulk viscosity (non-dimensional): moderately dense (GHD) predictions as a function of (a) overall volume fraction and (b) restitution coefficient. See legends presented in Figure 1. The dimensionless inputs are as follows: $m_1/m_2 = 8$, $\sigma_1/\sigma_2 = 2$, and $\phi_1/\phi = 0.5$.

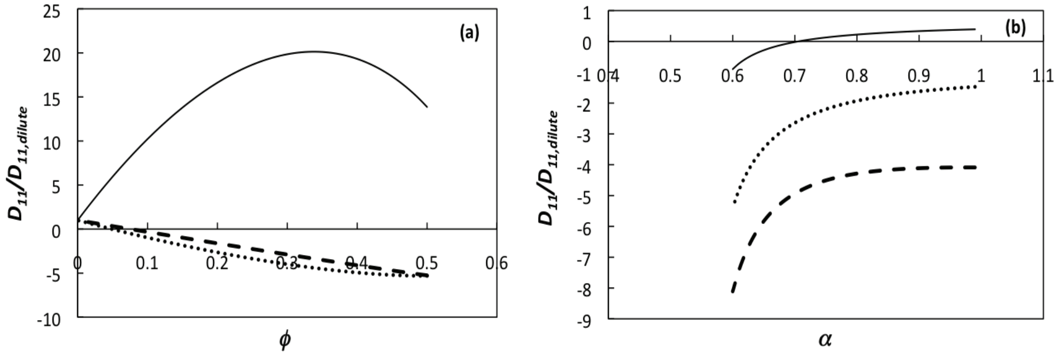

FIG. 6: Mutual diffusion (D_{11}): ratio of moderately dense (GHD) to dilute (GD) predictions as a function of (a) overall volume fraction and (b) coefficient of restitution. See legends presented in Figure 1.

C. Mass flux: Mutual diffusion, thermal diffusion

The mutual and thermal diffusion coefficients (D_{ij}, D_i^T) are elements of the constitutive equation for the mass flux. Based on the identities given by Eq. (2.5), the dimensionless mutual diffusion can be described by two quantities ($D_{11}/D_{11,\mathrm{dilute}}$ and $D_{22}/D_{22,\mathrm{dilute}}$), whereas the dimensionless thermal diffusion can be described by a single quantity ($D_1^T/D_{1,\mathrm{dilute}}^T$). Note that the dilute (GD) mutual and thermal diffusion coefficients presented by Garzó and Dufty

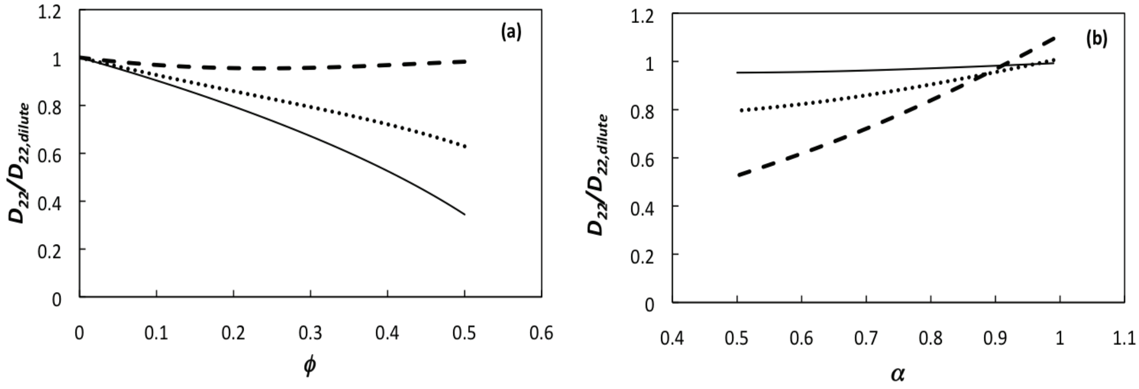

FIG. 7: Mutual diffusion (D_{22}): ratio of moderately dense (GHD) to dilute (GD) predictions as a function of (a) overall volume fraction and (b) coefficient of restitution. See legends presented in Figure 1.

[25] are defined using different spatial gradients than those used in the dense (GHD) theory and shown in Eq. (2.1). Nonetheless, a conversion is made such that both dense and dilute theories use the same representations for the fluxes, namely those shown in Sec. II of this paper, thereby ensuring an apples-to-apples comparison.

An examination of the dense-to-dilute ratio of the mutual diffusion coefficient elements (Figures 6 and 7) reveals a more complicated behavior of these quantities. Because $D_{11,\mathrm{dilute}}$ approaches zero for inelastic systems (at $\alpha \sim 0.52$), the coefficient of restitution was varied between 0.6 and 0.99 (Fig. 6b). As shown in Figure 6a, $D_{11}/D_{11,\mathrm{dilute}}$ is non-monotonic with respect to the volume fraction in less elastic systems ($\alpha = 0.5$), reaching a maximum ratio between the dense and dilute predictions of 20 at a volume fraction of 0.37. As the system becomes more elastic, $D_{11}/D_{11,\mathrm{dilute}}$ shifts from positive to negative. A change in the sign, as well as magnitude, between dense and dilute predictions of the mutual diffusion coefficient D_{11} may provide insight into counter intuitive species segregation [7, 9, 14, 15].

The results for $D_{22}/D_{22,\mathrm{dilute}}$, which are displayed in Figure 7, reveal increasing discrepancies between predictions as volume fraction increases and restitution coefficient decreases. In other words, GHD and GD theories display a larger discrepancy in denser, less elastic systems. For a relatively inelastic and dense system ($\alpha = 0.5$ and $\phi = 0.5$), the GHD prediction is about half of its dilute counterpart (Fig. 7a). However, it is significant to note the minor differences that exist between the dense and dilute predictions for the mutual diffusion coefficient D_{22} near the elastic limit ($\alpha = 0.9$) over a range of volume fractions from $\phi = 10^{-8}$ to 0.5 (Fig. 7a, $D_{22}/D_{22,\mathrm{dilute}} \sim 1$). GHD and GD theories display a larger discrepancy in denser, less elastic systems. For a relatively inelastic and dense system ($\alpha = 0.5$, $\phi = 0.4$), the moderately dense-phase theory prediction is about half of its dilute counterpart (Fig. 7a). Comparing dense- and dilute-phase predictions for the individual elements D_{11} and D_{22} shows the relative importance of each contribution to the mutual diffusion. At a moderately low volume fraction and high coefficient of restitution ($\phi = 0.1$, $\alpha = 0.9$), the discrepancies for GHD and GD theory predictions are about 70% and 5% for D_{11} and D_{22}, respectively. The dilute theory does not consider the finite size of the particles, which is the main difference between dense and dilute predictions. The discrepancy between D_{11} and $D_{11,\mathrm{dilute}}$ is larger than the discrepancy between D_{22} and $D_{22,\mathrm{dilute}}$ because D_{11} is directly related to the size of species 1, whereas D_{22} is proportional to the size of species 2 (recall $\sigma_1/\sigma_2 = 2$ for the case examined). Neither dilute quantity contains species size, therefore, the self-diffusion coefficient of a relatively large particle compared to its dilute counterpart will be greater than that of its smaller counterpart.

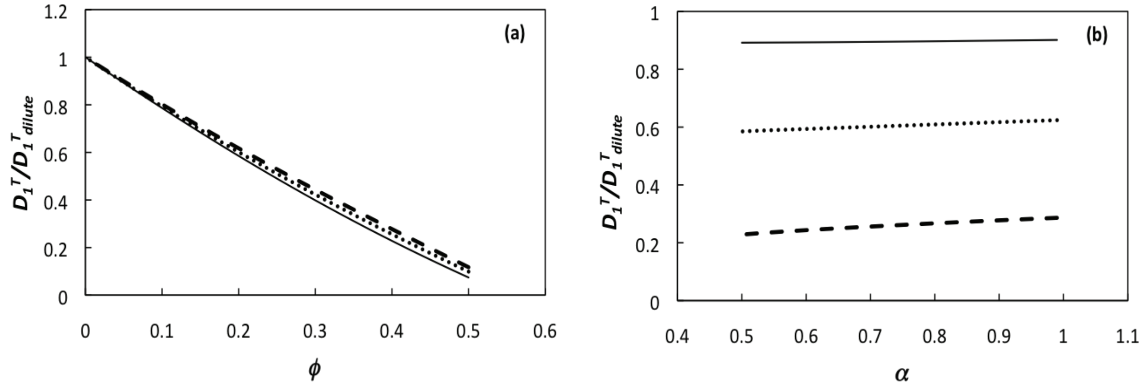

FIG. 8: Thermal diffusion: ratio of moderately dense (GHD) to dilute (GD) predictions as a function of (a) overall volume fraction and (b) coefficient of restitution. See legends presented in Figure 1.

The results for thermal diffusion (Figure 8) indicate that the ratio of dense-to-dilute predictions is extremely sensitive to changes in volume fraction compared to the coefficient of restitution. These general trends were also observed in the cooling rate and momentum flux relations (Figures 1, 3-5). The quantity $D_1^T/D_{1,\mathrm{dilute}}^T$ is nearly linear when plotted as a function of volume fraction, regardless the restitution coefficient (Fig. 8a). In a moderately dense system ($\phi = 0.4$), the results of Fig. 8a indicate that the dilute (GD) theory prediction of D_1^T is 5 times larger than predicted by GHD theory. At a much lower volume fraction of 0.1, the dilute (GD) theory prediction is larger than the moderately dense-phase (GHD) theory prediction by 20% (Fig. 8a).

D. Heat flux: thermal conductivity, Dufour coefficients

Heat flux is characterized by the thermal conductivity λ and the Dufour coefficients $D_{q,i}$. Figure 9 shows that the dense-to-dilute ratio of thermal conductivity increases monotonically with respect to both volume fraction and

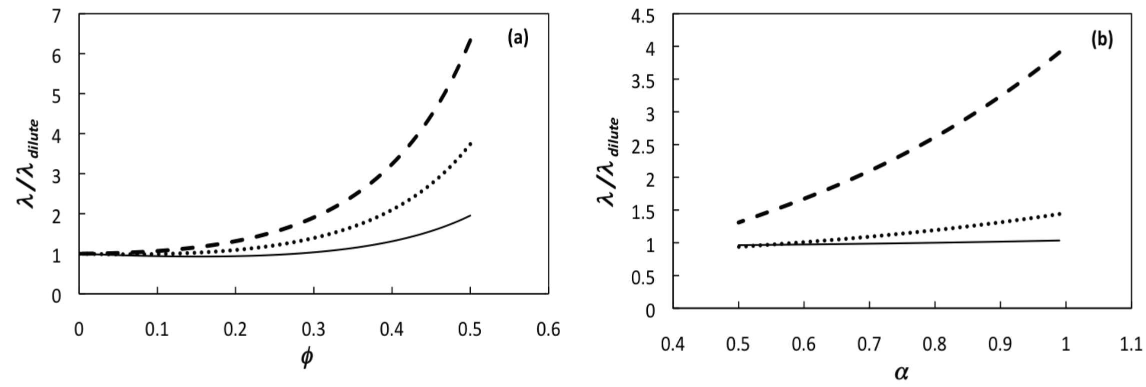

FIG. 9: Thermal Conductivity: ratio of moderately dense (GHD) to dilute (GD) predictions as a function of (a) overall volume fraction and (b) coefficient of restitution. See legends presented in Figure 1.

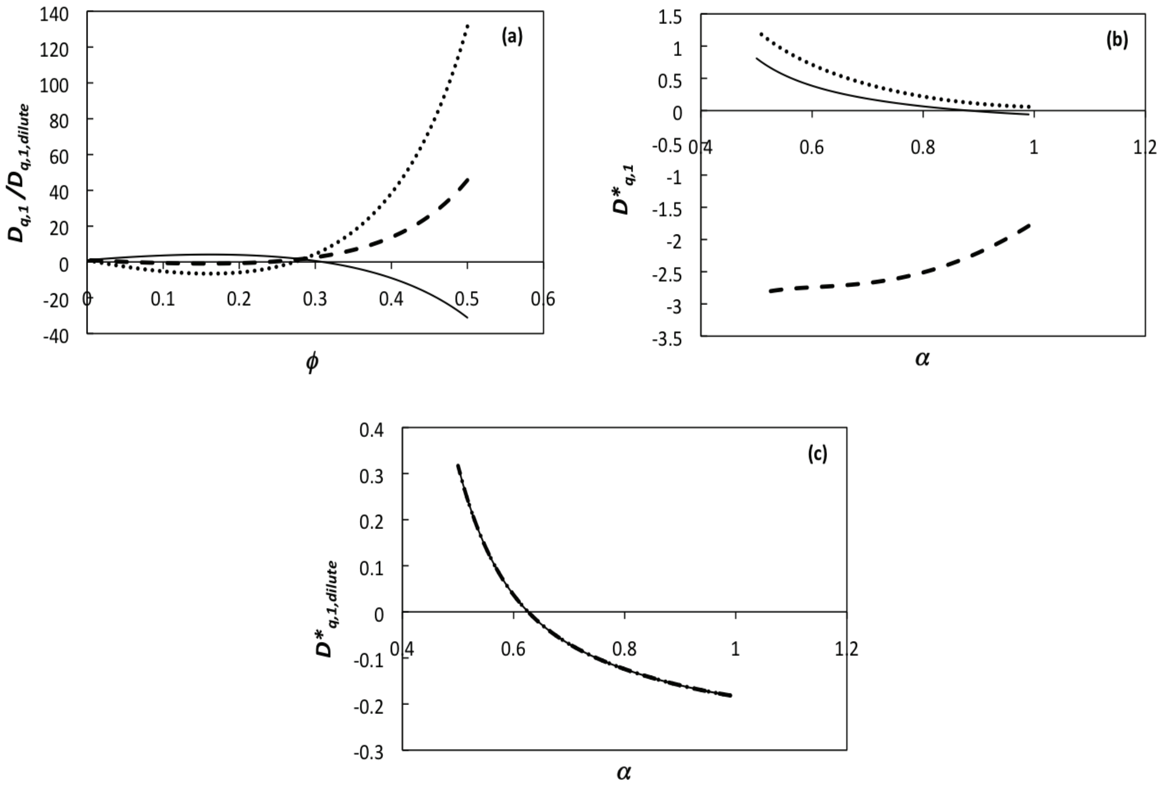

FIG. 10: Fig. 10. Dufour coefficient ($D_{q,1}$): (a) ratio of moderately dense (GHD) to dilute (GD) predictions as a function of overall volume fraction (b) dimensionless moderately dense (GHD) predictions as a function of coefficient of restitution (c) dimensionless dilute (GD) predictions as a function of coefficient of restitution. See legends presented in Figure 1. The dimensionless inputs are as follows: $m_1/m_2 = 8$, $\sigma_1/\sigma_2 = 2$, and $\phi_1/\phi = 0.5$.

coefficient of restitution. In an elastic, moderately dense system ($\phi \sim 0.4$), results (Fig. 9a) indicate that the prediction of thermal conductivity from GHD theory is 4 times larger than that of its dilute (GD) counterpart. For systems of lower densities ($\phi = 0.1$), the discrepancies range from 1% ($\alpha = 0.9$) to 6% ($\alpha = 0.5$) (Fig. 9a).

Similar to the mutual diffusion coefficient, the dilute form of the Dufour coefficient takes on a zero value at certain α, thereby making the dense-to-dilute value diverge at this value of α. Because this value occurs at a practical value of $\alpha = 0.63$ (whereas $D_{11,\text{dilute}}$ diverges at $\alpha = 0.52$), the dense and dilute predictions of the dimensionless Dufour coefficient $D^*_{q,1}$ were instead plotted separately against the coefficient of restitution (Figs. 10b and 10c), with the non-dimensionalization defined in Eq. (2.4). As expected, the dilute prediction of the Dufour coefficient is independent of

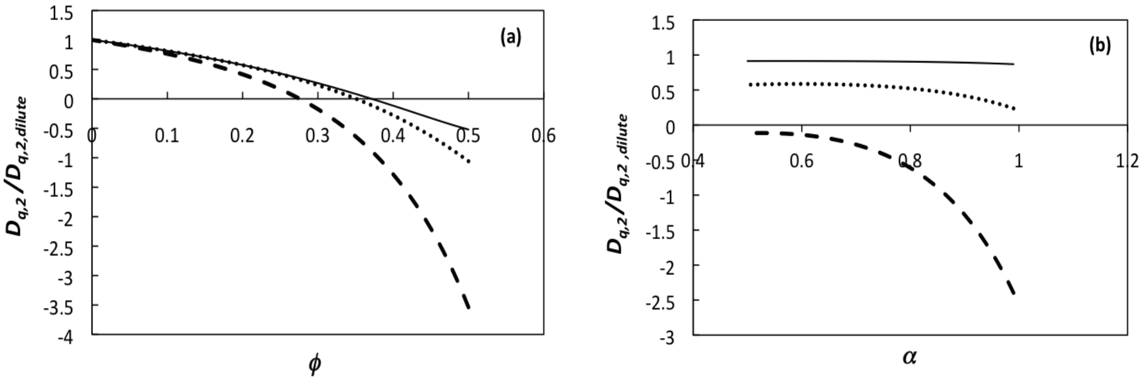

FIG. 11: Dufour coefficient ($D_{q,2}$): ratio of moderately dense (GHD) to dilute (GD) predictions as a function of (a) overall volume fraction and (b) coefficient of restitution. See legends presented in Figure 1.

the volume fraction (Fig. 10c).

The differences in magnitude between dilute and moderately dense predictions are non-trivial for both $D_{q,1}$ and $D_{q,2}$. More specifically, the discrepancies that exist between the predictions of $D_{q,1}$ and $D_{q,1,\text{dilute}}$ are up to 2 orders of magnitude in some cases (Figure 10). For a moderately dense, inelastic system ($\phi = 0.5$, $\alpha = 0.7$), the dense-phase prediction is over 100 times greater than its dilute counterpart (Fig. 10a). Even at a much lower volume fraction ($\phi = 0.01$), the discrepancy between dense and dilute predictions is at least 30%. The differences between dense and dilute predictions of $D_{q,2}$, shown in Figure 11, are less pronounced than $D_{q,1}$, however, still quite significant. In fact, results indicate at least a 20% discrepancy between predictions at a volume fraction $\phi = 0.1$ (Fig. 11a). As for the mutual and thermal diffusion coefficients, the dilute (GD) Dufour coefficient presented in Ref. [25] is defined using different spatial gradients than those used in the dense (GHD) theory and shown in Eq. (2.2). As done before, a conversion has been applied to compare the Dufour coefficients by using the same representation for the heat flux.

V. SUMMARY

To date, the understanding of particle segregation within polydisperse, rapid granular flows is somewhat limited due to a wide array of complexities that arise during the associated derivation of continuum theories. As previously mentioned, the two most common simplifications used in previous theories have been a Maxwellian velocity distribution and an equipartition of energy. This study focuses on two particular theories, neither of which assumes the above conditions. The first was proposed by Garzó and Dufty [25, 26] for binary, dilute mixtures (referred to as GD theory), and the second was recently proposed by Garzó, Hrenya and Dufty [28, 29] for binary, moderately dense mixtures (referred to as GHD theory). In order to gauge the importance of this dense-phase extension, the transport coefficients and equations of state predicted by GHD theory were compared to their dilute counterparts (GD theory). Furthermore, although not the focus of this study, it is worthwhile to mention that the CPU time required to evaluate the dense-phase coefficients was typically three times the requirement for its dilute counterpart.

A systematic comparison was carried out for three different cases (equal size and different mass, equal mass and different size, and different size and mass) over a range of mixture parameters (diameter ratio, mass ratio, and volume fraction ratio), the details of which are listed in Table 2. Though this study focuses on a case of different-sized species with the same material density, similar trends were observed for all other cases analyzed. Results indicate that transport coefficients and equations of state predicted by GHD theory are substantially different than those predicted by dilute (GD) theory. Also, significant differences between predictions were reported for fairly dilute systems ($\phi = 0.1$). In particular, the discrepancy between predictions was found to be as large as an order of magnitude. Certain coefficients, namely the mutual diffusion coefficient D_{11}, revealed that the magnitude and sign were different for the two theories. Naturally, the level of desired accuracy may vary between users of the theories. If, for example, 5% deviation between the GHD and GD predictions is deemed acceptable, then the need for a dense-phase correction is quite evident since the vast majority of quantities predicted by GHD theory are either larger or smaller than GD theory predictions by the 5% limit. Nonetheless, it is worthwhile to point that the comparison of dense- and dilute-phase predictions for a binary mixture presented here are independent of flow geometry. It is expected that is some flow geometries, one or more of the transport coefficients may dominate, while in other geometries another coefficient(s) may dominate. Such differences are system-dependent and should be taken into account when using the results contained herein.

Given the importance of the dense-phase corrections on the equations of state and transport coefficients, several follow-on studies are warranted: application of the theory to segregating systems in order to better understand the dominant segregation mechanisms (some previous studies have been carried in the tracer limit [14–16]), comparison with experimental and/or molecular-dynamics simulation data for purposes of validation, and application of the theory to a continuous particle size distribution. It is worthwhile to note that the GHD theory has been incorporated recently into the open-source, public MFIX code (https://mfix.netl.doe.gov/) for the case of binary mixtures, thereby increasing its availability to a wider class of researchers.

Acknowledgments

J.A.M. and C.M.H. are grateful for the funding support provided by the Department of Energy (DE-FC26-07NT43098) and the National Science Foundation (CBET-0318999). The research of V.G. has been supported by the Ministerio de Educación y Ciencia (Spain) through grant No. FIS2010-16587, partially financed by FEDER funds and by the Junta de Extremadura (Spain) through Grant No. GRU10158.

Appendix A: Corrections to previous results

In this Appendix we explicitly state some changes we have made in the original papers [28] and [29] to correct several errors and/or misprints we have found while working the present manuscript. With these changes, the interested reader can easily obtain the complete set of equations for the mass, heat and momentum fluxes and the cooling rate displayed along Section II.

Now, we list the changes affecting both papers:

- In Eq. (6.18) of Ref. [28], the term $n_\ell \partial_{n_j} \ln \chi_{i\ell}^{(0)}$ appearing in the second line of the right hand side of this equation must be replaced by $n_j \partial_{n_j} \ln \chi_{i\ell}^{(0)}$. This change affects to Eq. (C6) of Ref. [29] so that, its left hand side should read

  $$\sum_{\ell=1}^{s} n_\ell \chi_{i\ell}^{(0)} \sigma_{i\ell}^{d} \left(n_j \frac{\partial \ln \chi_{i\ell}^{(0)}}{\partial n_j} + I_{i\ell j} \right)$$

  Equations (2.7) and (2.8) can be derived after considering these changes.

- A factor "3" and the diameter σ_{ij} are missing in the expression (F25) of Ref. [28] in the collisional contribution to the heat flux. Thus, the third and fourth lines of the right hand side of this equation become

  $$+\frac{24B_2}{2+d} n_i \left(\frac{2\mu_{ji}}{m_j} \mathbf{q}_j^k - (d+2) \frac{T_i^{(0)}}{m_i m_j} \left(2\mu_{ij} - \mu_{ji} \right) \mathbf{j}_{0j}^{(1)} \right) + \sigma_{ij} C_{ij}^T \nabla \ln T + \sigma_{ij} \sum_{p=1}^{s} C_{ijp}^T \nabla \ln n_p \Bigg],$$

  where $\mu_{ij} \equiv m_i/(m_i + m_j)$. These changes also affect to Eqs. (7.14)-(7.16) of Ref. [28] and to Eqs. (3.37)-(3.39) of Ref. [29](collisional contributions to the heat flux transport coefficients). Taking into these changes, one gets Eqs. (2.17) and (2.20) of the present paper.

- The first line of the right hand side of Eq. (3.61) of Ref. [29] must be corrected. It should be given by

  $$\overline{d}_{q,ij} = -\frac{d+2}{2} \frac{n_i n_j T_i^3}{m_i T^2} \left(\frac{m_j}{\rho T_i} \sum_{\ell=1}^{s} m_\ell \frac{\omega_{i\ell} - \zeta^{(0)} \delta_{i\ell}}{n_\ell T_\ell} D_{\ell j} - \frac{2}{d+2} \frac{m_i T}{n_i T_i^3} \frac{\partial \zeta^{(0)}}{\partial n_j} \lambda_i - \frac{1}{d T_i} \frac{\partial \ln T_i}{\partial n_j} \right) + \cdots$$

  Equation (B10) of the present paper can be obtained after this change.

- In Eq. (2.16) of Ref. [29], the right hand side should read

  $$\frac{2}{d(d+2) n_i} \overline{e}_{i,D}$$

- A minus sign lacks on the second line of Eq. (2.19) of Ref. [29]. Thus, this line should read

$$= -\frac{\pi^{d/2}}{4d\Gamma\left(\frac{d}{2}\right)}\sum_{j=1}^{s} n_i n_j \chi_{ij}^{(0)} \cdots$$

- In Eq. (2.20) of Ref. [29], the term $e_{i,D}$ should be inside the summation sign. Moreover, the partial densities $n_i n_j$ must be also included inside the summation sign. Thus, the first line of Eq. (2.20) should read

$$\zeta^{(1,1)} = \frac{3\pi^{(d-1)/2}}{4d\Gamma\left(\frac{d}{2}\right)}\frac{v_0^3}{nT}\sum_{i=1}^{s}\sum_{j=1}^{s} n_i n_j e_{i,D}\sigma_{ij}^{d-1}\chi_{ij}^{(0)} \cdots$$

  Equation (2.42) of the present paper can be easily obtained after taking account these changes for the cooling rate.

- The summation $\sum_{j=1}^{s}$ is missing on the right hand side of Eq. (3.34) of Ref. [29].
- On the right hand side of Eqs. (A28) and (A29) of Ref. [29], the term $1+\alpha_{ij}$ should be changed to $1+\alpha_{ii}$.
- The ratio m_ℓ/m_i on the left hand side of Eq. (3.21) of Ref. [29] should be removed.
- In Eq. (A12) of Ref. [29], the factor $d+5$ near the end of the second line should be replaced by the factor $d+3$.
- The right hand side of Eq. (3.54) of Ref. [29] should read

$$\lambda^k = \sum_{i=1}^{s}\ \lambda_i^k = \sum_{i=1}^{s}\ \lambda_i + \ldots$$

Appendix B: Some explicit expressions

The kinetic part of the transport coefficients $D_{q,i}$ and λ are given by Eqs. (2.15) and (2.16), respectively. The (dimensionless) Sonine coefficients λ_i^* are defined by the matrix equation

$$\begin{pmatrix} \gamma_{11}^* - 2\zeta^* & \gamma_{12}^* \\ \gamma_{21}^* & \gamma_{22}^* - 2\zeta^* \end{pmatrix} \cdot \begin{pmatrix} \lambda_1^* \\ \lambda_2^* \end{pmatrix} = \begin{pmatrix} \overline{\lambda}_1^* \\ \overline{\lambda}_2^* \end{pmatrix}, \tag{B1}$$

where

$$\overline{\lambda}_i^* = \frac{m_1+m_2}{m_i} x_i \gamma_i^2 \sum_{j=1}^{2}\left(\delta_{ij} - \frac{\omega_{ij}^* - \zeta^*\delta_{ij}}{x_j\gamma_j} D_j^{*T} + \frac{\pi^{d/2}}{d(d+2)\Gamma\left(\frac{d}{2}\right)} n\sigma_2^d M_{ij} x_j (\sigma_{ij}/\sigma_2)^d \chi_{ij}\frac{\gamma_j}{\gamma_i} A_{ij}\right). \tag{B2}$$

The expressions of the (reduced) collision frequencies γ_{ij}^* and ω_{ij}^* can be found in the Appendix A of Ref. [29]. Moreover, in Eq. (A2) we have introduced the quantity

$$A_{ij} = (d+2)(M_{ij}^2 - 1) + (2d - 5 - 9\alpha_{ij})M_{ij}M_{ji} + (d - 1 + 3\alpha_{ij} + 6\alpha_{ij}^2)M_{ji}^2 + 6\frac{m_i T_j}{m_j T_i} M_{ji}^2 (1+\alpha_{ij})^2. \tag{B3}$$

The solution to Eq. (A1) is elementary and gives

$$\lambda_1^* = \frac{(\gamma_{22}^* - 2\zeta^*)\overline{\lambda}_1^* - \gamma_{12}^*\overline{\lambda}_2^*}{4\zeta^{*2} - 2(\gamma_{11}^* + \gamma_{22}^*)\zeta^* - \gamma_{12}^*\gamma_{21}^* + \gamma_{11}^*\gamma_{22}^*}, \quad \lambda_2^* = \frac{(\gamma_{11}^* - 2\zeta^*)\overline{\lambda}_2^* - \gamma_{21}^*\overline{\lambda}_1^*}{4\zeta^{*2} - 2(\gamma_{11}^* + \gamma_{22}^*)\zeta^* - \gamma_{12}^*\gamma_{21}^* + \gamma_{11}^*\gamma_{22}^*}. \tag{B4}$$

With these results the kinetic part λ^{k*} can be written as

$$\lambda^{k*} = \frac{\overline{\lambda}_1^*(\gamma_{22}^* - 2\zeta^* - \gamma_{21}^*) + \overline{\lambda}_2^*(\gamma_{11}^* - 2\zeta^* - \gamma_{12}^*)}{4\zeta^{*2} - 2(\gamma_{11}^* + \gamma_{22}^*)\zeta^* - \gamma_{12}^*\gamma_{21}^* + \gamma_{11}^*\gamma_{22}^*} + \left(\frac{\gamma_1}{M_{12}} - \frac{\gamma_2}{M_{21}}\right) D_1^{T*}. \tag{B5}$$

The kinetic part of the transport coefficients $D_{q,i}^{k*}$ is given in terms of the Sonine coefficients $d_{q,ij}^*$. By using matrix notation, the coupled set of four equations for the coefficients

$$\left\{d_{q,11}^*, d_{q,12}^*, d_{q,21}^*, d_{q,22}^*\right\} \tag{B6}$$

can be written as

$$\Lambda_{\mu\mu'}X_{\mu'}=Y_\mu. \tag{B7}$$

Here, X_μ is the column matrix defined by the set (A6) and $\Lambda_{\mu\mu'}$ is the square matrix

$$\Lambda_{\mu\mu'}=\left(\begin{array}{cccc}\gamma_{11}^*-\frac{3}{2}\zeta^* & 0 & \gamma_{12}^* & 0\\ 0 & \gamma_{11}^*-\frac{3}{2}\zeta^* & 0 & \gamma_{12}^*\\ \gamma_{21}^* & 0 & \gamma_{22}^*-\frac{3}{2}\zeta^* & 0\\ 0 & \gamma_{21}^* & 0 & \gamma_{22}^*-\frac{3}{2}\zeta^*\end{array}\right). \tag{B8}$$

The column matrix Y is

$$\mathbf{Y}=\left(\begin{array}{c}\overline{d}_{q,11}^*\\ \overline{d}_{q,12}^*\\ \overline{d}_{q,21}^*\\ \overline{d}_{q,22}^*\end{array}\right), \tag{B9}$$

where

$$\begin{aligned}\overline{d}_{q,ij}^* \;=\;& \frac{m_1+m_2}{m_i}x_i\gamma_i n_j\frac{\partial\gamma_i}{\partial n_j}-\frac{m_1+m_2}{m_i}x_ix_j\gamma_i^2\sum_{\ell=1}^2\frac{\omega_{i\ell}^*-\zeta^*\delta_{i\ell}}{x_\ell\gamma_\ell}D_{\ell j}^*+\frac{n_j}{\nu_0}\frac{\partial\zeta^{(0)}}{\partial n_j}\lambda_i^*\\ &+\frac{\pi^{d/2}}{d(d+2)\Gamma\left(\frac{d}{2}\right)}\frac{m_1+m_2}{m_i}x_i\gamma_i^2 n\sigma_2^d\sum_{\ell=1}^2 M_{\ell i}x_\ell(\sigma_{i\ell}/\sigma_2)^d\chi_{i\ell}(1+\alpha_{i\ell})\\ &\times\left\{\left[\delta_{j\ell}+\frac{1}{2}\left(n_j\frac{\partial\chi_{i\ell}}{\partial n_j}+I_{i\ell j}\right)\right]B_{i\ell}+\frac{m_i}{m_\ell\gamma_i}n_j\frac{\partial\gamma_\ell}{\partial n_j}A_{i\ell}\right\}.\end{aligned} \tag{B10}$$

In Eq. (A10), A_{ij} is defined by Eq. (B3) and B_{ij} is given by

$$\begin{aligned}B_{ij} \;=\;& (d+8)M_{ij}^2+(7+2d-9\alpha_{ij})M_{ij}M_{ji}+(2+d+3\alpha_{ij}^2-3\alpha_{ij})M_{ji}^2+3M_{ji}^2(1+\alpha_{ij})^2\frac{m_i^2T_j^2}{m_j^2T_i^2}\\ &+\left[(d+2)M_{ij}^2+(2d-5-9\alpha_{ij})M_{ij}M_{ji}+(d-1+3\alpha_{ij}+6\alpha_{ij}^2)M_{ji}^2\right]\frac{m_iT_j}{m_jT_i}\\ &-(d+2)\left(1+\frac{m_iT_j}{m_jT_i}\right).\end{aligned} \tag{B11}$$

The solution to Eq. (A7) provides the expressions of $d_{q,ij}^*$. The result is

$$d_{q,11}^*=\frac{4\overline{d}_{q,21}^*\gamma_{12}^*-4\overline{d}_{q,11}^*\gamma_{22}^*+6\overline{d}_{q,11}^*\zeta^*}{4\gamma_{12}^*\gamma_{21}^*+(2\gamma_{11}^*-3\zeta^*)(3\zeta^*-2\gamma_{22}^*)},\quad d_{q,12}^*=\frac{4\overline{d}_{q,22}^*\gamma_{12}^*-4\overline{d}_{q,12}^*\gamma_{22}^*+6\overline{d}_{q,12}^*\zeta^*}{4\gamma_{12}^*\gamma_{21}^*+(2\gamma_{11}^*-3\zeta^*)(3\zeta^*-2\gamma_{22}^*)}. \tag{B12}$$

The kinetic part $D_{q,1}^{k*}$ can be easily obtained when one takes into account Eqs. (2.15) and (A10). The result is

$$D_{q,1}^{k*}=\frac{4\gamma_{12}^*(\overline{d}_{q,21}^*+\overline{d}_{q,22}^*)+2(\overline{d}_{q,11}^*+\overline{d}_{q,12}^*)(3\zeta^*-2\gamma_{22}^*)}{4\gamma_{12}^*\gamma_{21}^*+(2\gamma_{11}^*-3\zeta^*)(3\zeta^*-2\gamma_{22}^*)}+\left(\frac{\gamma_1}{M_{12}}-\frac{\gamma_2}{M_{21}}\right)x_1D_{11}^*. \tag{B13}$$

The expressions of $d_{q,22}^*$, $d_{q,21}^*$ and $D_{q,2}^{k*}$ can be obtained from Eqs. (B12) and (B13), respectively, by interchanging 1↔2.

In order to get the dependence of the transport coefficients on the parameters of the system, one needs to know the explicit forms of χ_{ij} and μ_i. For hard disks ($d=2$), a good approximation for the pair correlation function χ_{ij} is [17]

$$\chi_{ij}=\frac{1}{1-\phi}+\frac{9}{16}\frac{\phi}{(1-\phi)^2}\frac{\sigma_i\sigma_jM_1}{\sigma_{ij}M_2}, \tag{B14}$$

where

$$M_n = \sum_{s=1}^{2} x_s \sigma_s^n. \tag{B15}$$

The expression of the chemical potential μ_i of the species i consistent with the approximation (B14) is [36]

$$\begin{aligned}\frac{\mu_i}{T} &= \ln(\lambda_i^2 n_i) - \ln(1-\phi) + \frac{M_1}{4M_2}\left[\frac{9\phi}{1-\phi} + \ln(1-\phi)\right]\sigma_i \\ &\quad -\frac{1}{8}\left[\frac{M_1^2}{M_2^2}\frac{\phi(1-10\phi)}{(1-\phi)^2} - \frac{8}{M_2}\frac{\phi}{1-\phi} + \frac{M_1^2}{M_2^2}\ln(1-\phi)\right]\sigma_i^2,\end{aligned} \tag{B16}$$

where $\lambda_i(T)$ is the (constant) de Broglie's thermal wavelength [37]. In the case of hard spheres ($d = 3$), we take for the pair correlation function χ_{ij} the following approximation [38]

$$\chi_{ij} = \frac{1}{1-\phi} + \frac{3}{2}\frac{\phi}{(1-\phi)^2}\frac{\sigma_i\sigma_j M_2}{\sigma_{ij} M_3} + \frac{1}{2}\frac{\phi^2}{(1-\phi)^3}\left(\frac{\sigma_i\sigma_j M_2}{\sigma_{ij} M_3}\right)^2. \tag{B17}$$

The chemical potential consistent with (B17) is [37]

$$\begin{aligned}\frac{\mu_i}{T} &= \ln(\lambda_i^3 n_i) - \ln(1-\phi) + 3\frac{M_2}{M_3}\frac{\phi}{1-\phi}\sigma_i + 3\left[\frac{M_2^2}{M_3^2}\frac{\phi}{(1-\phi)^2} + \frac{M_1}{M_3}\frac{\phi}{1-\phi} + \frac{M_2^2}{M_3^2}\ln(1-\phi)\right]\sigma_i^2 \\ &\quad -\left[\frac{M_2^3}{M_3^3}\frac{\phi(2-5\phi+\phi^2)}{(1-\phi)^3} - 3\frac{M_1M_2}{M_3^2}\frac{\phi^2}{(1-\phi)^2} - \frac{1}{M_3}\frac{\phi}{1-\phi} + 2\frac{M_2^3}{M_3^3}\ln(1-\phi)\right]\sigma_i^3.\end{aligned} \tag{B18}$$

Appendix C: Expressions for a low-density granular binary mixture

In this Appendix we include the explicit expressions of the transport coefficients and the cooling rate for a *dilute* binary granular mixture. These expressions can be easily obtained from the results derived in Sec. II for a moderately dense binary mixture by taking the limit $n\sigma_2^d \to 0$.

1. Mass and heat flux transport coefficients

The expressions of the reduced coefficients D_1^{T*}, D_{11}^*, and D_{12}^* are given by

$$D_1^{T*} = (\nu_D^* - \zeta^*)^{-1}\left(x_1\gamma_1 - \frac{\rho_1}{\rho}\right), \tag{C1}$$

$$D_{11}^* = \left(\nu_D^* - \frac{1}{2}\zeta^*\right)^{-1}\left(\frac{D_1^{T*}}{x_1\nu_0}n_1\frac{\partial\zeta^{(0)}}{\partial n_1} - \frac{\rho_1}{\rho} + \gamma_1 + n_1\frac{\partial\gamma_1}{\partial n_1}\right), \tag{C2}$$

$$D_{12}^* = \left(\nu_D^* - \frac{1}{2}\zeta^*\right)^{-1}\left(\frac{D_1^{T*}}{x_2\nu_0}n_2\frac{\partial\zeta^{(0)}}{\partial n_2} - \frac{\rho_1}{\rho} + n_1\frac{\partial\gamma_1}{\partial n_2}\right), \tag{C3}$$

where ν_D^* is given by Eq. (2.9) with $\chi_{12} = 1$. Upon deriving Eqs. (C1)–(C3), use has been made of the identities $p^* = 1$ and $\partial p/\partial n_i = T$.

The collisional transfer contributions to the heat flux transport coefficients vanish in the low density limit ($n\sigma_2^d \to 0$). Thus, only their kinetic contributions must be considered. In dimensionless forms, the thermal conductivity λ^* and the Dufour $D_{q,i}^*$ coefficients are

$$\lambda^* = \lambda_1^* + \lambda_2^* + \left(\frac{\gamma_1}{M_{12}} - \frac{\gamma_2}{M_{21}}\right)D_1^{T*}, \tag{C4}$$

$$D_{q,1}^* = d_{q,11}^* + d_{q,21}^* + \left(\frac{\gamma_1}{M_{12}} - \frac{\gamma_2}{M_{21}}\right) x_1 D_{11}^*, \quad D_{q,2}^* = d_{q,22}^* + d_{q,12}^* + \left(\frac{\gamma_1}{M_{12}} - \frac{\gamma_2}{M_{21}}\right) x_2 D_{12}^*, \tag{C5}$$

where the coefficients λ_i^* and $d_{q,ij}^*$ are given by Eqs. (B4) and (B12), respectively, with

$$\overline{\lambda}_i^* = \frac{m_1+m_2}{m_i} x_i \gamma_i^2 \sum_{j=1}^{2} \left(\delta_{ij} - \frac{\omega_{ij}^* - \zeta^* \delta_{ij}}{x_j \gamma_j} D_j^{*T}\right), \tag{C6}$$

$$\overline{d}_{q,ij}^* = \frac{m_1+m_2}{m_i} x_i \gamma_i n_j \frac{\partial \gamma_i}{\partial n_j} - \frac{m_1+m_2}{m_i} x_i x_j \gamma_i^2 \sum_{\ell=1}^{2} \frac{\omega_{i\ell}^* - \zeta^* \delta_{i\ell}}{x_\ell \gamma_\ell} D_{\ell j}^* + \frac{n_j}{\nu_0} \frac{\partial \zeta^{(0)}}{\partial n_j} \lambda_i^*. \tag{C7}$$

The dilute forms of the collision frequencies ω_{ij}^* and γ_{ij}^* can be obtained from their dense counterparts (Appendix A of Ref. [29]) by simply taking $\chi_{ij} = 1$.

2. Pressure tensor

In the low-density limit, the hydrostatic pressure $p = nT$, the bulk viscosity $\kappa = 0$ and the shear viscosity η has only kinetic contributions. It is given by $\eta = (p/\nu_0)\eta^*$ where $\eta^* = \eta_1^* + \eta_2^*$. The partial contributions η_i^* are given by Eqs. (2.30) and (2.31) with

$$\overline{\eta}_1 = x_1 \gamma_1, \quad \overline{\eta}_2 = x_2 \gamma_2. \tag{C8}$$

As before, the (reduced) collision frequencies τ_{ij}^* can be easily obtained from their corresponding dense forms by considering $\chi_{ij} = 1$.

3. Cooling rate

The first-order contribution ζ_u to the cooling rate ζ vanishes in the dilute case [see Eqs. (2.40)–(2.45)]. The dilute expression for the coefficient $\zeta^{(0)} = \zeta_i^{(0)}$ can be obtained from Eq. (2.38) by taking $\chi_{ij} = 1$.

[1] S. Savage, in Developments in Engineering Mechanics, edited by A. P. S. Selvadurai, Elsevier, Amsterdam, 1987, pp. 347-363.
[2] J. Bridgwater, in Granular Matter: An Interdisciplinary Approach, edited by A. Metha, Springer, Berlin, 1994, pp. 161–194.
[3] J. Ottino, D. Khakhar, Mixing and segregation of granular materials, Ann. Rev. Fluid Mech. 32 (2000) 55-91.
[4] IUTAM Symposium on Segregation in Granular flows, edited by A.D. Rosato, D.L. Blackmore, Kluwer, Dordrecht, 2000.
[5] C. M. Hrenya, Kinetic theory for granular materials: Polydispersity, in Computational Gas-Solids Flows and Reacting Systems: Theory, Methods and Practice, edited by S. Pannala, M. Syamlal, T. OrBrien, IGI Global, Hershey, PA. In press.
[6] S. Hsiau, M. Hunt, Granular thermal diffusion in flows of binary-sized mixtures, Acta Mechanica 114 (1996) 121-137.
[7] J. J. Brey, M. J. Ruiz-Montero, F. Moreno, Energy partition and segregation for an intruder in a vibrated granular system under gravity, Phys. Rev. Lett. 95 (2005) 098001.
[8] J. Galvin, S. Dahl, C. Hrenya, On the role of non-equipartition in the dynamics of rapidly flowing granular mixtures, J. Fluid Mech. 528 (2005) 207-232.
[9] V. Garzó, Segregation in granular binary mixtures: Thermal diffusion, Europhys. Lett. 75 (2006) 521-527.
[10] M. Schröter, S. Ulrich, J. Kreft, S. B. Swift, H. L. Swinney, Mechanisms in the size segregation of a binary granular mixture, Phys. Rev. E 74 (2006) 011307.
[11] R. Wildman, J. Jenkins, P. Krouskop, J. Talbot, A comparison of the predictions of a simple kinetic theory with experimental and numerical results for a vibrated granular bed consisting of nearly elastic particles of two sizes, Phys. Fluids 18 (2006) 073301.
[12] D. K. Yoon, J. T. Jenkins, The influence of different species granular temperatures on segregation in a binary mixture of dissipative grains, Phys. Fluids 18 (2006) 073303.
[13] X. Liu, M. Metzger, B. Glasser, Couette flow with a bidisperse particle mixture, Phys. Fluids 19 (2007) 073301.
[14] V. Garzó, Brazil-nut effect versus reverse Brazil-nut effect in a moderately granular dense gas, Phys. Rev. E 78 (2008) 020301(R).
[15] V. Garzó, Segregation by thermal diffusion in moderately dense granular mixtures, Eur. Phys. J. E 29 (2009) 261-274.

[16] V. Garzó, F. Vega Reyes, Mass transport of impurities in a moderately dense granular gas, Phys. Rev. E 79 (2009) 041303.

[17] J. Jenkins, F. Mancini, Balance laws and constitutive relations for plane flows of a dense, binary mixture of smooth, nearly elastic, circular disks, J. Appl. Mech. 54 (1987) 27.

[18] V. Mathiesen, T. Solberg, H. Arastoopour, B.H. Hjertager, Experimental and computational study of multiphase gas/particle flow in a CFB riser, AIChE Journal 45 (1999) 2503-2518 (1999).

[19] L. Huilin, D. Gidaspow, E. Manger, Kinetic theory of fluidized binary granular mixtures, Phys. Rev. E 64 (2001) 061301.

[20] M. F. Rahaman, J. Naser, P.J Witt, An unequal granular temperature kinetic theory: Description of granular flow with multiple particle classes, Powder Technol. 138 (2003) 82-92.

[21] H. Iddir, H. Arastoopour, Modeling of multitype particle flow using the kinetic theory approach, AIChE Journal 51 (2005) 1620-1632.

[22] J. Jenkins, F. Mancini, Kinetic theory for binary mixtures of smooth, nearly elastic spheres, Phys. Fluids A 1 (1989) 2050-2057.

[23] B. Arnarson, J. T. Willits, Thermal diffusion in binary mixtures of smooth, nearly elastic spheres with and without gravity, Phys. Fluids 10 (1998) 1324-1328.

[24] S. Chapman, T. G. Cowling, The Mathematical Theory of Nonuniform Gases, Cambridge University Press, Cambridge, 1970.

[25] V. Garzó, J. W. Dufty, Hydrodynamics for a granular mixture at low density, Phys. Fluids 14 (2002) 1476-1490.

[26] V. Garzó, J. M. Montanero, J. W. Dufty, Mass and heat fluxes for a binary granular mixture at low density, Phys. Fluids 18 (2006) 083305.

[27] V. Garzó, J. M. Montanero, Navier-Stokes transport coefficients of d-dimensional granular binary mixtures at low density, J. Stat. Phys. 129 (2007) 27.

[28] V. Garzó, J. W. Dufty, C. M. Hrenya, Enskog theory for polydisperse granular mixtures. I. Navier-Stokes order transport, Phys. Rev. E 76 (2007) 031303.

[29] V. Garzó, C. M. Hrenya, J. W. Dufty, Enskog theory for polydisperse granular mixtures. II. Sonine polynomial approximation, Phys. Rev. E 76 (2007) 031304.

[30] A. Goldshtein, M. Shapiro, Mechanics of collisional motion of granular materials. Part 1. General hydrodynamic equations, J. Fluid Mech. 282 (1995) 75-114.

[31] J. J. Brey, J. W. Dufty, A. Santos, Dissipative dynamics for hard spheres, J. Stat. Phys. 87 (1997) 1051-1066.

[32] M. López de Haro, E.G.D. Cohen, J. Kincaid, The Enskog theory for multicomponent mixtures. I. Linear transport theory, J. Chem. Phys. 78 (1983) 2746-2759.

[33] H. van Beijeren, M. H. Ernst, The non-linear Enskog-Boltzmann equation, Phys. Lett. A 43 (1973) 367-368; The modified Enskog equation for mixtures, Physica 70 (1973) 225-242.

[34] V. Garzó, J. M. Montanero, Shear viscosity for a moderately dense granular binary mixture, Phys. Rev. E 68 (2003) 041302.

[35] V. Garzó, J. W. Dufty, Homogeneous cooling state for a granular mixture, Phys. Rev. E 60 (1999) 5706-5713.

[36] A. Santos, private communication.

[37] T. M. Reed, K. E. Gubbins, Applied Statistical Mechanics, McGraw-Hill, New York, 1973, Chap. 6.

[38] T. Boublik, Hard-Sphere equation of state, J. Chem. Phys. 53 (1970) 471-472 (1970); E. W. Grundke, D. Henderson, Distribution functions of multi-component fluid mixtures of hard spheres, Mol. Phys.24 (1972) 269-281; L. L. Lee, D. Levesque, Perturbation theory for mixtures of simple liquids, Mol. Phys. 26 (1973) 1351-1370.